J Clust Sci (2015) 26:211–221
DOI 10.1007/s10876-014-0729-x

ORIGINAL PAPER

Photoinduced Electron Transfer Reactions of Hexarhenium(III) Cluster: Oxidative Quenching of $[Re_6S_8Cl_6]^{4-}$ Emission by Electron Acceptors

Noboru Kitamura · Natsuki Kobayashi · Shoji Ishizaka · Takashi Yoshimura · Haeng-Boo Kim · Yoichi Sasaki

Received: 9 April 2014 / Published online: 18 May 2014

Abstract The photoredox ability of a hexarhenium(III) cluster, $[Re_6(\mu_3\text{-}S)_8Cl_6]^{4-}$, in acetonitrile was examined on the basis of the emission quenching experiments of the cluster by a series of neutral organic electron acceptors (*A*). The photoinduced electron transfer quenching rate constants and the relevant activation parameters demonstrated that the hexarhenium(III) cluster acted as a useful photoredox sensitizer towards various *A* and the system gave a high charge separation yield owing to electrostatic repulsion between the product ions: $[Re_6(\mu_3\text{-}S)_8Cl_6]^{3-}$ and A^-. These results were proved explicitly by nanosecond transient absorption spectroscopy.

Keywords Hexarhenium(III) cluster · Photoinduced electron transfer · Charge separation

Electronic supplementary material The online version of this article (doi:10.1007/s10876-014-0729-x) contains supplementary material, which is available to authorized users.

N. Kitamura (✉) · N. Kobayashi · S. Ishizaka · T. Yoshimura · H.-B. Kim · Y. Sasaki
Department of Chemistry, Faculty of Science, Hokkaido University, Sapporo 060-0810, Japan
e-mail: kitamura@sci.hokudai.ac.jp

Present Address:
S. Ishizaka
Department of Chemistry, Graduate School of Science, Hiroshima University, Kagamiyama, Higashi-Hiroshima 739-8526, Japan

Present Address:
T. Yoshimura
Radioisotope Research Center, Osaka University, Suita 565-0871, Japan

Present Address:
H.-B. Kim
Department of Chemistry, Faculty of Science, Ibaraki University, 2-1-1 Bunkyo, Mito, Ibaraki 310-8512, Japan

Introduction

Photoinduced electron transfer (PET) reactions are the fundamental basis of chemical conversion of light energy as well as of synthetic organic photochemistry, and the related studies have been conducted extensively among the past decades [1, 2]. For photocatalytic reactions by redox sensitizers, transition metal complexes are widely employed. In particular, polypyridine ruthenium(II) complexes (RuL_3^{2+}, L = polypyridine or polydiazine ligand) have been studied extensively [1–4], since the complexes in general possess absorption in the visible region and long excited state lifetime in solution at room temperature. Furthermore, it is well known that some of RuL_3^{2+} possesses strong reduction and oxidation abilities towards various substrates: electron acceptors (*A*) and donors (*D*) [1–4]. In practice, various RuL_3^{2+} complexes represented by $Ru(bpy)_3^{2+}$ (bpy = 2,2′-bipyridine) have been shown to be potential photoredox sensitizers [1–7]. It is worth emphasizing that, however, it is certainly true that PET reactions of RuL_3^{2+} with *D* give rise to high ion product yields, while those with *A* do not afford free ions efficiently (i.e., RuL_3^{3+} and A^-). This is simply because that oxidative quenching of RuL_3^{2+} by *A* produces electrostatically-attractive ion pair (RuL_3^{3+} and A^-), while reductive quenching affords an electrostatically repulsive RuL_3^{+}–D^+ pair [5–7]. For constructing efficient photoredox systems, therefore, the electrostatic interaction in a product ion pair is worth considering and studying in detail.

We reported previously, on the other hand, that hexarhenium(III) clusters, $[Re_6(\mu_3\text{-}S)_8X_6]^{4-}$ (*X* = Cl^-, Br^-, I^-, and so forth), showed relatively intense room temperature emission in the visible ∼ near infrared region (600–1,000 nm) with the emission lifetime (τ) and quantum yield (Φ) in acetonitrile being τ = 4–11 μs and Φ = 0.015–0.056, respectively [8]. Later, several research groups have reported that various $[Re_6E_8L_6]^z$ (*E* = S, Se, or Te; *L* = *X* [8–11], CN [11–13], OH/H_2O [12–14], NCS [15], N-heteroaromatics [16–21], phosphine derivatives [17, 18, 22, 23], HCOO [24], CH3COO [25], and N_3 [26],) clusters showed intense and long-lived emission in solution and solid phases at room temperature. It is worth noting that the τ values of the some of $[Re_6E_8L_6]^z$ clusters in deaerated acetonitrile are much longer (τ = 4–11 μs) than that of $Ru(bpy)_3^{2+}$ (τ = 850 ns in acetonitrile at 298 K). As another unique characteristics, furthermore, $[Re_6E_8L_6]^z$ possesses a strong reducing ability. As a typical example, the oxidation potential of $[Re_6S_8Cl_6]^{4-}$ (=$[Re_6]^{4-}$) in acetonitrile is +0.27 V (vs. saturated calomel electrode (SCE)) and, thus, the redox ability of $[Re_6]^{4-}$ is remarkable [20, 27, 28]. Owing to the long excited-state lifetime and the strong redox ability, $[Re_6]^{4-}$ is thus expected to act as an efficient photoredox sensitizer in various systems. For oxidative quenching of the excited triplet state of $[Re_6]^{4-}$ by a neutral electron acceptor (*A*), in particular, the negative charges on the cluster suggest very strong electrostatic repulsion between the product ions, $[Re_6]^{3-}$ and A^-, and, thus, the system enables a high charge separation yield. A detailed study on PET emission quenching of $[Re_6]^{4-}$ by electron acceptors would thus contribute to further progresses in the photoredox chemistry of transition metal complexes. In this paper, we demonstrate that $[Re_6S_8Cl_6]^{4-}$ undergoes efficient PET reactions with various electron acceptors in acetonitrile [29].

Experimental

Chemicals

$[Re_6S_8Cl_6]^{4-}$ abbreviated as $[Re_6]^{4-}$ used in this study was the same sample reported earlier [8, 29]. Acetonitrile (Wako Pure Chemicals Co. Ltd.) as a medium throughout the study was purified by distillation over CaH_2. Organic electron acceptors (A) were purchased from Tokyo Kasei Co. Ltd.: for the numbering of *A*, see Table 1. 4-Nitroanisole (**1**), 3-nitroanisole (**5**), methyl 3-nitrobenzoate (**6**), or 1,4-benzoquinone (**12**) was recrystallized from *n*-hexane, an aqueous methanol, methanol, or petroleum ether, respectively. 2,3,5,6-Tetramethyl-1,4-dinitrobenzene (**2**), 3,4-dimethylnitrobenzene (**3**), 3,5-dimethylnitrobenzene (**4**), methyl 4-nitrobenzoate (**7**), and 1,3-dinitrobenzene (**8**) were purified by recrystallization from ethanol. Tetrachlorophathalic anhydride (**9**) and tetrachloro-1,4-benzoquinone (**13**) were recrystallized from acetone. 1,4-Naphthoquinone (**10**) and pyromellitic dianhydride (**11**) were purified by recrystallization from ethanol and 1,4-doxane, respectively, followed by vacuum sublimation. Pyrene (Wako Pure Chemicals Co. Ltd.) was purified successively by column chromatography (silica gel, *n*-hexane:chloroform = 1:2) and vacuum sublimation.

Emission Spectroscopy and Other Measurements

Steady-state emission quenching experiments of $[Re_6]^{4-}$ by *A* in CH_3CN at a given temperature (*T*) were performed with a Hitachi F-4500 spectrofluorometer. Emission lifetime measurements were conducted by using a Nd^{3+}:YAG laser (Continum Surelite II, 355 nm, $\sim$6 ns pulse-width) as an excitation light source and a streak camera system (Hamamatsu Photonics, C4334) as a photodetector. In both cases, sample temperature was controlled within 1 °C (13–58 °C) by circulating thermostated water to a sample cell holder by using a thermo-electronic controller (Hitachi 250-0346 or Yamato-Komatsu COOLNICS CTE42A). Sample solutions were deaerated thoroughly by purging an Ar-gas stream over 20 min and sealed at the constriction of a cell prior to the experiments. Cyclic voltammetry of $[Re_6]^{4-}$ or *A* in CH_3CN was carried out by using an electrochemical analyzer (ALS, model 701A) with tetra-*n*-butylammonium hexafluorophosphate (0.1 M) as a supporting electrolyte.

Nanosecond Time-Resolved Absorption Spectroscopy

Nanosecond 355-nm laser pulses mentioned above were used for excitation of a sample solution. Timing between the laser and a pulsed Xe lamp as a monitoring light source (150 W, Tokyo Instruments Inc.) was controlled by a digital delay generator (DG535, Stanford Research Systems Inc.) and the transient absorption spectrum was measured by a gated multichannel photodiode detector (SMA, Princeton Instruments Inc.) equipped with a polychromator (Jovin-Yvon HR-320).

Table 1 PET emission quenching of $[Re_6S_8Cl_6]^{4-}$ by neutral electron acceptors (*A*) in acetonitrile

	Electron acceptors (*A*) ($E(A/A^-)$ V. vs. SCE)	ΔG_{23} kcal/mol (eV)	k_q M/s ($RT\ln k_q$)	ΔG_{23}* kcal/mol	ΔH_{23}* kcal/mol	ΔS_{23}* cal/mol deg
1.	4-Nitroanisole (−1.27)	−4.4 (−0.19)	3.5×10^8 (0.505)	5.8	2.8	−10.1
2.	2,3,5,6-Tetramethyl-1,4-dinitrobenzene (−1.27)	−4.4 (−0.19)	4.4×10^7 (0.452)	7.1	4.6	−8.3
3.	3,4-Dimethylnitrobenzene (−1.24)	−5.1 (−0.22)	2.4×10^8 (0.496)	6.3	2.5	−11.7
4.	3,5-Dimethylnitrobenzene (−1.20)	−6.0 (−0.26)	2.7×10^8 (0.499)	5.9	3.0	−9.9
5.	3-Nitroanisole (−1.14)	−7.4 (–0.32)	1.0×10^9 (0.533)	5.2	2.4	−9.2
6.	Methyl 3-nitrobenzoate (−1.06)	−9.2 (−0.40)	3.1×10^9 (0.562)	4.5	1.3	−10.8
7.	Methyl 4-nitrobenzoate (−0.95)	−11.8 (−0.51)	6.4×10^9 (0.580)	4.1	0.9	−10.6
8.	1,3-Dinitrobenzene (−0.92)	–12.5 (–0.54)	2.5 x 10^{10} (0.615)	3.1	0.7	−7.9
9.	Tetrachlorophthalic anhydride (−0.84)	−14.3 (−0.62)	7.6×10^9 (0.585)	4.0	1.0	−10.1
10.	1,4-Naphthoquinone (−0.69)	−17.8 (−0.77)	3.4×10^{10} (0.623)	3.0	−0.1	−10.5
11.	Pyromellitic dianhydride (−0.53)	–21.5 (−0.93)	1.3×10^{10} (0.599)	3.9	1.4	−8.6
12.	1,4-Benzoquinone (−0.51)	−21.9 (−0.95)	5.7×10^{10} (0.636)	2.8	0.5	−8.0
13.	Tetrachloro-1,4-benzoquinone (+0.02)	−34.1(−1.48)	3.2×10^{10} (0.622)	3.2	−0.2	−11.4

Determination of the Quenching Rate Constant and Other Parameters

The PET reaction of $[Re_6]^{4-}$ with *A* in acetonitrile is assumed to proceed by the several steps as shown in Scheme 1 [6, 29, 30]. Upon photoexcitation of $[Re_6]^{4-}$, the excited triplet state of $[Re_6]^{4-}$ ($^*[Re_6]^{4-}$) undergoes diffusional encounter with *A* (the rate constant of k_{12}) and this produces the encounter complex, $[^*[Re_6]^{4-}\cdots A]$. k_{21} is the dissociation rate constant of the encounter complex and, k_{23} and k_{32} are the forward and backward electron transfer rate constants within the contact ion pair, $[[Re_6]^{3-}\cdots A^-]$, respectively. $[[Re_6]^{3-}\cdots A^-]$ as the PET product undergoes either dissociation to free ions (k_{34}, $[Re_6]^{3-}$ and A^-) or back electron transfer to the ground state (k_{30}).

A bimolecular quenching rate constant (k_o) in CH_3CN at a given temperature (*T*) was determined by the slope value of the Stern–Volmer plot on the basis of emission intensity or lifetime measurements. For the emission intensity quenching experiments, the emission lifetime of $[Re_6]^{4-}$ in the absence of *A* (τ) at a given *T* was determined by separate experiments. Every emission decay determined at around 700 nm obeyed a single exponential function in the *T* range of 13–58 °C, which was used to calculate k_o at a given *T*. Since k_o determined by the emission intensity measurements agreed very well with that by the emission lifetime

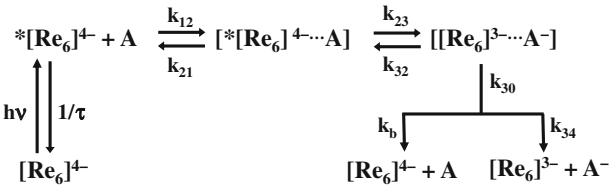

Scheme 1 PET reaction of $[Re_6S_8Cl_6]^{4-}$ (=$[Re_6]^{4-}$) with *A* in a polar solvent

measurements irrespective of *A*, the quenching reaction of $[Re_6]^{4-}$ by *A* was concluded to proceed in a dynamic pathway.

Since k_o includes the contributions from both the diffusional and electron transfer steps, a correction for the diffusional effect on k_o was made by Eq. 1,

$$k_q^{-1} = k_o^{-1} - k_{12}^{-1} \tag{1}$$

where k_q represent the corrected activation-controlled quenching rate constant. The k_{12} value was calculated by the Smoluchowski equation, Eq. 2,

$$k_{12} = \frac{2RT}{3000\eta}\left[2 + \frac{r_{Re}}{r_A} + \frac{r_A}{r_{Re}}\right] \tag{2}$$

where r_A and r_{Re} are the radii of *A* (3.8 Å) and $[Re_6]^{4-}$ (5.5 Å), respectively. R and η represent the gas constant and the viscosity of CH_3CN, respectively.

Results and Discussion

Kinetic Analysis of PET Emission Quenching of $[Re_6S_8Cl_6]^{4-}$ by Neutral Organic Electron Acceptors

The emission from $[Re_6]^{4-}$ in acetonitrile was quenched efficiently in the presence of *A*. As the k_q data at 298 K were summarized in Table 1, the value increased from 10^7 to 10^{10} $M^{-1}s^{-1}$ in the decreasing order of the reduction potential of *A*. To discuss further the point, we evaluated the Gibbs free energy change for the forward electron transfer step, ΔG_{23}, on the basis of the oxidation potential of $[Re_6]^{4-}$ ($E([Re_6]^{3-}/[Re_6]^{4-}) = +0.27$ V vs. SCE), the reduction potential of *A* ($E(A/A^-)$ vs. SCE, see Table 1), and the excited triplet state energy of $[Re_6]^{4-}$ ($E^{em} = 1.61$ eV, the emission energy at 298 K) as in Eq. 3,

$$\Delta G_{23} = E([Re_6]^{3-}/[Re_6]^{4-}) - E(A/A^-) - E^{em} + w_p - w_r \tag{3}$$

where w_p or w_r is the electrostatic work necessary to bring two product ions or two initial reactants together to the close-contact distance ($d = r_A + r_{Re}$), respectively, and is given by Eq. 4.

$$w_r = w_p = \frac{Z_a Z_b e^2}{\varepsilon d} \tag{4}$$

In Eq. 4, Z_a and Z_b are the charge numbers of the two reactants for w_r and those of the two product ions for w_p and, e and ε are the elemental electron charge and the static dielectric constant of CH_3CN (37.5), respectively. In the present experiments, since we used neutral quenchers throughout the study, w_r was zero and $w_p = -0.12$ V. The ΔG_{23} value calculated for each A is included in Table 1. It is clear that the ΔG_{23} values are sufficiently negative (i.e., exoergonic) for all quenchers and the k_q value increases with a negative increase in ΔG_{23}. The results are readily understood by PET emission quenching of $[Re_6]^{4-}$.

According to the Scheme 1 and Bock et al. [30], k_q can be expressed as in Eq. 5,

$$k_q = K_{12} k_{23} \frac{k_{30}}{k_{30} + k_{32}} \tag{5}$$

where K_{12} is the formation constant of the encounter complex and can be calculated by the Fuoss–Eigen equation, Eq. 6,

$$K_{12} = \frac{4\pi N d^3}{3000} \exp(-w_r/RT) \tag{6}$$

where N is the Avogadro number and K_{12} is calculated to be 2.03 M^{-1} for the Re^{4-}—neutral quencher systems ($w_r = 0$ and $d = 9.3$ Å) at 298 K. When the transition-state theory is applied to the forward electron transfer step (k_{23}), Eq. 5 can be rewritten as in Eq. 7,

$$k_q = K_{12} \nu_{23} F \exp(-\Delta G_{23}^*/RT) \tag{7}$$

where ν_{23} is the frequency factor of the k_{23} step (assumed to be 10^{12} s^{-1}) and $F = k_{30}/(k_{30} + k_{32})$. ΔG_{23}* is the Gibbs activation free energy for the electron transfer step and is given by the Marcus theory [31], Eq. 8,

$$\Delta G_{23}^* = \frac{\lambda}{4}\left[1 + \frac{\Delta G_{23}}{\lambda}\right]^2 \tag{8}$$

where λ represents the sum of the inner—(λ_i) and outer-sphere reorganization energies (λ_o). Combining Eqs. 7 and 8, we obtain Eq. 9.

$$k_q = K_{12} \nu_{23} F \exp\left[-\frac{\lambda}{4}\left(1 + \frac{\Delta G_{23}}{\lambda}\right)^2 / RT\right] \tag{9}$$

When $k_{30} \gg k_{32}$, Eq. 5 can be simplified to Eq. 10.

$$k_q = K_{12} k_{23} \tag{10}$$

By combining Eqs. 9 and 10, furthermore, k_q in a natural logarithmic form is given by Eq. 11 at $|\Delta G_{23}| \ll 2\lambda$.line feed, similar to "Case II" Case I

$$RT \ln k_q = RT \ln(K_{12} \nu_{23}) - \frac{\lambda}{4} - \frac{\Delta G_{23}}{2} \tag{11}$$

When $k_{30} \ll k_{32}$ and $F = k_{30}/k_{32}$ in Eq. 5, on the other hand, we obtain Eq. 12,

$$k_q = K_{12} K_{23} k_{30} \tag{12}$$

where $K_{23} = k_{23}/k_{32}$. Similar treatment of Eq. 12 with that obtaining Eq. 11 gives Eq. 13.

Case II

$$RT \ln k_q = RT \ln k_q K_{12} - \Delta G_{23} \tag{13}$$

Eqs. 11 and 13 indicate that the slope value of the RTlnk_q vs. ΔG_{23} plot should be -0.5 when the product ions, $[[Re_6]^{3-} \cdots A^-]$, undergoes efficient charge separation (k_{34}) or back electron transfer to the ground state (k_{30}) (Case I, $k_{30} \gg k_{32}$), while that is -1.0 if the k_{32} process dominates to k_{30} (Case II, $k_{30} \ll k_{32}$).

Figure 1 shows the relationship between the lnk_q and ΔG_{23} values. At $\Delta G_{23} < -0.8$ eV, the RTlnk_q value levels off at the diffusion-limited rate constant value, while that increases with a negative increase in ΔG_{23} in $-0.2 > \Delta G_{23} > -0.7$ eV. It is worth emphasizing that the slope value of the plot in $-0.2 > \Delta G_{23} > -0.7$ eV is -0.48, demonstrating the PET emission quenching of $[Re_6]^{4-}$ by A proceeds by the Case I mechanism (i.e., $k_{30} \gg k_{32}$). Since k_{30} includes the rate constant of charge separation to $[Re_6S_8Cl_6]^{3-}$ and the anion radical of A (A^-, k_{34}) as well as the back electron transfer rate constant to the ground state reactants (k_b, see Scheme 1), the present kinetic analysis does not necessarily provide direct evidence for the charge separation to $[Re_6]^{3-}$ and A^-. To discuss further the point, therefore, we conducted the T dependence of the PET emission quenching and transient absorption spectroscopy of the $[Re_6]^{4-} - A$ system.

Temperature Dependence of PET Emission Quenching of $[Re_6S_8Cl_6]^{4-}$ by A

We studied the T (285–331 K) dependence of PET emission quenching of $[Re_6]^{4-}$ by 13 electron acceptors in CH_3CN. The activation free energy (ΔG_{23}*), activation enthalpy (ΔH_{23}*), and activation entropy (ΔS_{23}*) thus determined by the Eyring plots (ln(k_q/T) vs. T^{-1}) are included in Table 1.

As seen in Table 1, a negative increase in ΔG_{23} from -4.4 to -34.1 kcal/mol rendered the decreases in both ΔG_{23}* (from 6–7 to $\sim$3 kcal/mol) and ΔH_{23}* (from 3–4 to 0.5–1.0 kcal/mol), while ΔS_{23}* was remained almost constant at $-8 \sim -11$ eu (=cal/mol deg) irrespective of ΔG_{23}: $T\Delta S_{23}$* $= -2.4 \sim -3.3$ kcal/mol at 298 K. Such results remind us the T dependence of reductive quenching of $Ru(bpy)_3^{2+}$ (= $[Ru]^{2+}$) by aromatic amines (D) [5], in which the analogous ΔG_{23} dependences of the activation parameters with those determined in the present study have been observed. In the case of oxidative quenching of $[Ru]^{2+}$ by A [6], on the other hand, a negative increase in ΔG_{23} resulted in apparent negative ΔH_{23}* values and a large decrease in ΔS_{23}*. The results for PET quenching of $[Ru]^{2+}$ have been explained in terms of the electrostatic interaction in the product ion pair, $[[R_6u]^{3+} \cdots A^-]$. For a $[Ru]^{2+} - D$ system, namely, the electrostatic interaction between the product ions is repulsive ($[[Ru]^+ \cdots D^+]$) and, this usually leads to the ΔG_{23} dependences of the activation parameters as described above. On the other hand, since the PET reaction of a $[Ru]^{2+} - A$ system produces an electrostatically–attractive ion pair ($[[Ru]^{3+} \cdots A^-]$), back electron transfer from the ion pair to the excited state encounter complex proceeds very efficiently, rendering an apparent negative ΔH_{23}* value and a large decrease in ΔS_{23}* of the quenching, as reported in

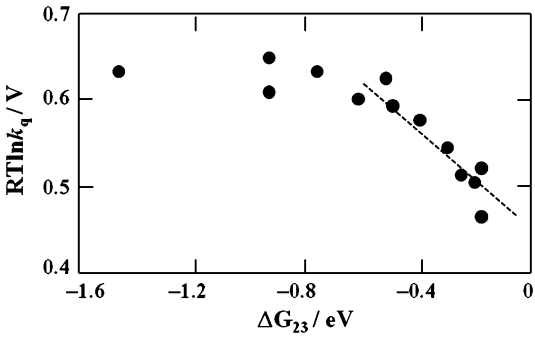

Fig. 1 A relationship between RTlnk_q and ΔG_{23} for PET emission quenching of $[Re_6S_8Cl_6]^{4-}$ by *A* in CH_3CN at 298 K

detail previously [5–7]. Since oxidative quenching of the excited triplet state of $[Re_6]^{4-}$ by *A* produces an electrostatically–repulsive product ion pair ($[[Re_6]^{3-}\cdots A^-]$), the analogous *T* dependences of the activation parameters with those for reductive quenching of $[Ru]^{2+}$ is quite reasonable. Thus, it can be concluded that the PET reaction of a $[Re_6]^{4-} - A$ system undergoes by the Case I mechanism (i.e., $k_{30} \gg k_{32}$), which agrees very well with the conclusion of the kinetic analysis of the data in Fig. 1.

Transient Absorption Spectrocopy of $[Re_6S_8Cl_6]^{4-}$: Pyromellitic Dianhydride (PDA) System

To obtain the direct evidence for the charge separation process of a $[Re_6]^{4-} - A$ system, we conducted nanosecond transient absorption spectroscopy. As a typical example, the transient absorption spectrum of a $[Re_6]^{4-}$—pyromellitic dianhydride (PDA) system in CH_3CN at 298 K observed during the first 500 ns after laser excitation is shown in Fig. 2. In the $[Re_6]^{4-} -$ PDA system, we observed transient absorption in the wavelength (λ) region of 500–700 nm, which was assigned safely to the anion radical of PDA as reported by Hino et al. [32]. Unfortunately, however, we could not detect the absorption band of $[Re_6]^{3-}$ in the λ region studied. The time profile of the absorption band at $\lambda = 660$ nm is shown in Fig. 3. Figure 3 demonstrates clearly that the anion radical of PDA decays very slowly with the second-order kinetics and survives even at around 70 μs after laser excitation. Knowing the molar absorption coefficient (ε) of the absorption band at $\lambda = 660$ nm to be $\varepsilon = 3.8 \times 10^4$ /M/cm [32], we evaluated the decay time constant of the PDA anion radical to be 2.7×10^8 /M/s.

As a reference system producing an electrostatically-attractive product ion pair by PET, we also studied transient absorption of a pyrene (Py)—PDA system as shown in Fig. S1 in Supporting Information. As seen in Fig. S1, the absorption band of the Py cation radical was observed at around 445 nm in addition to the absorption bands of the anion radical of PDA. Both the anion radical of PDA and the cation radical of Py decayed by the second-order kinetics and the decay rate constants of the Py cation radical ($\varepsilon = 4.5 \times 10^4$ /M/cm at $\lambda = 445$ nm) and the PDA anion radical were 1.8×10^{10} and 1.4×10^{10} /M/s, respectively, whose values were

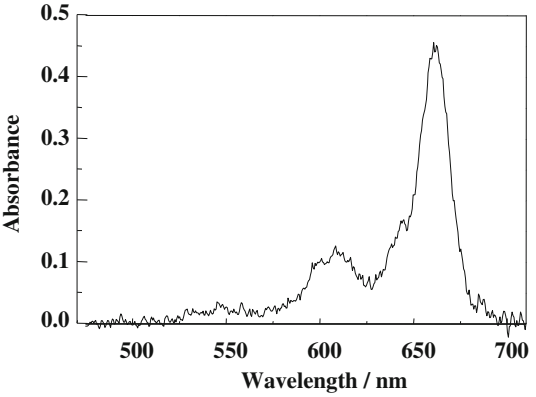

Fig. 2 Transient absorption spectrum (gate time = 500 ns) of the $[Re_6S_8Cl_6]^{4-}$ (5.3×10^{-4} M) − PDA (1.9×10^{-3} M) system in CH_3CN at 298 K

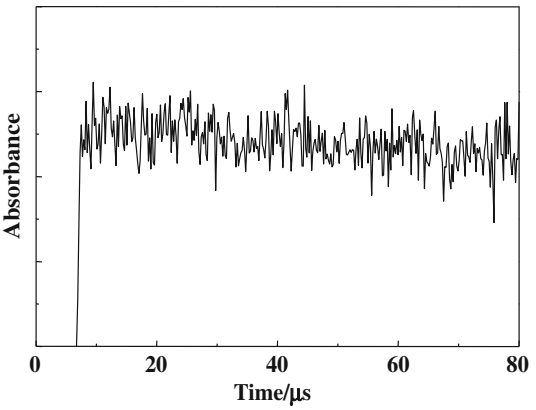

Fig. 3 Time profile of the absorbance of the PDA anion radical at 660 nm

50 ∼ 60 times faster than that of the PDA anion radical produced in the $[Re_6]^{4-}$ − PDA system. These results demonstrate explicitly that the electrostatic interaction between the product ions governs the charge separation yield and the lifetimes of the free ions produced by a PET reaction. In the present $[Re_6]^{4-}$ − A system, thus, the negative charges on $[Re_6]^{4-}$ plays decisive role in determining the reaction mechanism (Case I) and the charge separation yield of the PET reaction.

Conclusions

The present study demonstrated that hexarhenium(III) complex, $[Re_6S_8Cl_6]^{4-} = [Re_6]^{4-}$, possesses a high photoredox ability toward a neutral electron acceptor, as proven by the kinetic analysis of the PET emission quenching rate constant, the relevant activation parameters, and nanosecond transient absorption spectroscopy. It has been also demonstrated that the electrostatic interaction between the product ion pair produced by PET is the one of the important factors determining the charge separation yield of the product ion pair. Besides $[Re_6S_8Cl_6]^{4-}$, a number of negatively-charged hexarhenium(III) clusters

with different oxidation potentials have been hitherto reported and such clusters will be also acted as a strong photoredox sensitizer or catalyst.

References

1. M. A. Fox and M. Channon (eds.) *Photoinduced Electron Transfer*, vol. A–D (Elsevier, Amsterdam, 1988).
2. V. Balzani (ed.) *Electron Transfer in Chemistry*, vol. 1–5 (Wiley, Weinheim, 2001).
3. K. Kalyanasundaram (1983). *Coord. Chem. Rev.* **46**, 159.
4. K. Kalyanasundaram *Photochemistry of Polypyridine and Porphyrin Complexes* (Academic Press, London, 1992).
5. N. Kitamura, H.-B. Kim, S. Okano, and S. Tazuke (1989). *J. Phys. Chem.* **93**, 5750.
6. H.-B. Kim, N. Kitamura, Y. Kawanishi, and S. Tazuke (1989). *J. Phys. Chem.* **93**, 5757.
7. N. Kitamura, R. Obata, H.-B. Kim, and S. Tazuke (1989). *J. Phys. Chem.* **93**, 5764.
8. T. Yoshimura, S. Ishizaka, K. Umakoshi, Y. Sasaki, H.-B. Kim, and N. Kitamura (1999). *Chem. Lett.* **1999**, 697.
9. N. Kitamura, Y. Ueda, S. Ishizaka, K. Yamada, M. Aniya, and Y. Sasaki (2005). *Inorg. Chem.* **44**, 6308.
10. L. F. Szczepura, D. L. Cedeño, D. B. Johnson, R. McDonald, S. A. Knott, K. M. Jeans, and J. L. Durham (2010). *Inorg. Chem.* **49**, 11386.
11. T. Yoshimura, S. Ishizaka, Y. Sasaki, H.-B. Kim, N. Kitamura, N. G. Naumov, M. N. Sokolov, and V. E. Fedorov (1999). *Chem. Lett.* **1999**, 1121.
12. Y. V. Mironov, K. A. Brylev, S.-J. Kim, S. G. Kozlova, N. Kitamura, and V. E. Fedorov (2011). *Inorg. Chim. Acta* **370**, 363.
13. A. Y. Ledneva, K. A. Brylev, A. I. Smolentsev, Y. V. Mironov, Y. Molard, S. Cordier, N. Kitamura, and N. G. Naumov (2014). *Polyhedron* **67**, 351.
14. T. Yoshimura, Z.-N. Chen, A. Itasaka, M. Abe, Y. Sasaki, S. Ishizaka, N. Kitamura, S. S. Yaroboi, S. F. Solodovnikov, and V. E. Fedorov (2003). *Inorg. Chem.* **42**, 4857.
15. T. Yoshimura, K. Umakoshi, Y. Sasaki, S. Ishizaka, H.-B. Kim, and N. Kitamura (2000). *Inorg. Chem.* **39**, 1765.
16. T. G. Gray, C. M. Rudzinski, D. G. Nocera, and R. H. Holm (1999). *Inorg. Chem.* **38**, 5932.
17. T. G. Gray, C. M. Rudzinski, E. E. Meyer, R. H. Holm, and D. G. Nocera (2003). *J. Am. Chem. Soc.* **125**, 4755.
18. T. Yoshimura, S. Ishizaka, T. Kashiwa, A. Ito, E. Sakuda, A. Shinohara, and N. Kitamura (2011). *Inorg. Chem.* **50**, 9918.
19. T. Yoshimura, C. Suo, K. Tsuge, S. Ishizaka, K. Nozaki, Y. Sasaki, N. Kitamura, and A. Shinohara (2010). *Inorg. Chem.* **49**, 531.
20. Y. V. Mironov, K. A. Brylev, M. A. Shestopalov, S. S. Yarovoi, V. E. Fedorov, H. Spies, H.-J. Pietzsch, H. Stephan, G. Geipel, G. Bernhard, and W. Kraus (2006). *Inorg. Chim. Acta* **359**, 1129.
21. Z.-N. Chen, T. Yoshimura, M. Abe, Y. Sasaki, S. Ishizaka, H.-B. Kim, and N. Kitamura (2001). *Angew. Chem. Int. Ed.* **40**, 239.
22. Z.-N. Chen, T. Yoshimura, M. Abe, K. Tsuge, Y. Sasaki, S. Ishizaka, H.-B. Kim, and N. Kitamura (2001). *Chem. Eur. J.* **20**, 4447.
23. K. A. Brylev, Y. V. Mironov, S. S. Yarovoi, N. G. Naumov, V. E. Fedorov, S.-J. Kim, N. Kitamura, Y. Kuwahara, K. Yamada, S. Ishizaka, and Y. Sasaki (2007). *Inorg. Chem.* **46**, 7414.
24. K. A. Brylev, Y. V. Mironov, S. G. Kozlova, V. E. Fedorov, S.-J. Kim, H.-J. Pietzsch, H. Stephan, A. Ito, S. Ishizaka, and N. Kitamura (2009). *Inorg. Chem.* **48**, 2309.
25. K. A. Brylev, Y. V. Mironov, V. E. Fedorov, S.-J. Kim, H.-J. Pietzsch, H. Stephan, A. Ito, and N. Kitamura (2010). *Inorg. Chim. Acta* **363**, 2686.

26. A. Gandubert, K. A. Brylev, T. T. Nguyen, N. G. Naumov, N. Kitamura, Y. Molard, R. Gautier, and S. Cordier (2013). *Z. Anorg. Allg. Chem.* **639**, 1756.
27. T. Yoshimura, K. Umakoshi, Y. Sasaki, and A. G. Sykes (1999). *Inorg. Chem.* **38**, 5557.
28. T. Yoshimura (2000), Ph. D Thesis, Hokkaido University.
29. N. Kobayashi, S. Ishizaka, T. Yoshimura, H.-B. Kim, Y. Sasaki, and N. Kitamura (2000). *Chem. Lett.* **2000**, 234.
30. C. R. Bock, J. A. Connor, A. R. Gutierrez, T. J. Meyer, D. G. Whitten, B. P. Sullivan, and J. K. Nagle (1979). *J. Am. Chem. Soc.* **101**, 4815.
31. R. A. Marcus (1956). *J. Chem. Phys.* **24**, 966.
32. T. Hino, H. Akazawa, H. Masuhara, and N. Mataga (1976). *J. Phys. Chem.* **80**, 33.